# Autophagy promotes synapse development in *Drosophila*

Wei Shen and Barry Ganetzky

Laboratory of Genetics, University of Wisconsin-Madison, Madison, WI 53706

Autophagy, a lysosome-dependent degradation mechanism, mediates many biological processes, including cellular stress responses and neuroprotection. In this study, we demonstrate that autophagy positively regulates development of the *Drosophila melanogaster* larval neuromuscular junction (NMJ). Autophagy induces an NMJ overgrowth phenotype closely resembling that of *highwire* (*hiw*), an E3 ubiquitin ligase mutant. Moreover, like *hiw*, autophagy-induced NMJ overgrowth is suppressed by *wallenda* (*wnd*) and by a dominant-negative c-Jun $NH_2$-terminal kinase ($bsk^{DN}$). We show that autophagy promotes NMJ growth by reducing Hiw levels. Thus, autophagy and the ubiquitin–proteasome system converge in regulating synaptic development. Because autophagy is triggered in response to many environmental cues, our findings suggest that it is perfectly positioned to link environmental conditions with synaptic growth and plasticity.

## Introduction

Regulation of synaptic growth and plasticity is essential for proper development and function of neural circuits that underlie behavior and its modification in response to experience and environment. The *Drosophila melanogaster* larval neuromuscular junction (NMJ) is a powerful system for dissecting molecular mechanisms that mediate synaptic growth (Collins and DiAntonio, 2007). Previous studies have identified key positive and negative regulators of synaptic growth, including proteins associated with cell adhesion, the cytoskeleton, endocytosis, and Wnt and bone morphogenic protein signaling (Schuster et al., 1996; Aberle et al., 2002; Packard et al., 2002; Coyle et al., 2004; Koh et al., 2004; Marie et al., 2004; Dickman et al., 2006; Pack-Chung et al., 2007; Liebl et al., 2008; O'Connor-Giles et al., 2008; Rodal et al., 2008). The balance of opposing forces and the multiple layers of regulation that are imposed reveal that complex mechanisms have evolved to ensure correct synaptic size.

Protein degradation via the ubiquitin–proteasome system (UPS) is an important negative regulatory mechanism of NMJ growth, as revealed by striking overgrowth in *highwire* (*hiw*) mutants (Wan et al., 2000). Hiw, an E3 ubiquitin ligase, restrains synaptic growth primarily by down-regulation of Wallenda (Wnd), a MAPK kinase kinase (Collins et al., 2006).

Another major protein degradation mechanism is autophagy, which involves activation of the induction complex, formation of autophagosomes that engulf cytoplasmic materials, subsequent fusion of autophagosomes with lysosomes, and finally, degradation of sequestered material by lysosomal enzymes (Levine and Klionsky, 2004). Various stress conditions trigger autophagy, including starvation, hypoxia, high temperature, accumulation of protein aggregates, and infection (Hara et al., 2006; Nakai et al., 2007). The association of autophagy with human diseases such as neurodegeneration and cancer reveals its importance as a cellular surveillance system (Levine and Klionsky, 2004; Levine and Kroemer, 2008).

Because the UPS is an important negative regulator of NMJ development, we examined whether autophagy also plays a role. We discovered that autophagy positively regulates NMJ development and, remarkably, does so by controlling Hiw levels. Thus, autophagy and the UPS converge to regulate NMJ growth. Because autophagy is highly conserved, it is likely to play an important role in synapse development in more complex animals.

Correspondence to Barry Ganetzky: ganetzky@wisc.edu

Abbreviations used in this paper: ERK, extracellular signal-regulated kinase; Hiw, Highwire; NMJ, neuromuscular junction; UAS, upstream activating sequence; UPS, ubiquitin–proteasome system; Wnd, Wallenda.



The Rockefeller University Press $30.00
J. Cell Biol. Vol. 187 No. 1 71–79
www.jcb.org/cgi/doi/10.1083/jcb.200907109

## Results and discussion

### Autophagy promotes NMJ growth

Autophagy involves multiple steps, including induction, autophagosome formation, fusion of autophagosomes with lysosomes, and recycling of autophagy components. Disrupting any of these steps impairs autophagy. Several highly conserved *ATG* genes encoding core components of the autophagy machinery have been identified in yeast. Mutations in genes, including *atg1*, *-2*, *-6*, and *-18*, have also been isolated and characterized in *Drosophila* (Scott et al., 2004; Berry and Baehrecke, 2007). To assess the role of autophagy in NMJ development, we examined the effect of mutations in *atg* genes whose normal functions span the entire process: *atg1* is defective in autophagy induction, *atg6* is defective in autophagosome formation, and *atg2* and *-18* are defective in retrieval of other ATG proteins from autophagosomes (Levine and Kroemer, 2008). Regardless of the step impaired, all of these *atg* mutants exhibited significant reduction in NMJ size (Fig. 1, A and B). These results demonstrate that a basal level of autophagy is required to promote NMJ development.

Overexpression of $atg1^{+}$ is sufficient to induce high levels of autophagy in larval fat bodies and salivary glands (Berry and Baehrecke, 2007; Scott et al., 2007). If autophagy is a positive regulator of NMJ development, an increase in autophagy might enhance synaptic growth. Consistent with previous studies, panneuronal overexpression of *upstream activating sequence* (*UAS*)–$atg1^{+}$ under the control of *C155-Gal4* or *elav-Gal4* drivers induced high levels of autophagy in the nervous system, as indicated by increased staining with LysoTracker, an acidophilic dye which has been used to assess autophagy by labeling acidic structures, including lysosomes (Fig. 1 C; Berry and Baehrecke, 2007; Scott et al., 2007). Under these conditions, bouton number increased more than twofold (Fig. 1, D and E). To further verify that this NMJ overgrowth was caused by elevated autophagy rather than to some other effect of $atg1^{+}$ overexpression, we tested whether mutations in other *atg* genes suppress this phenotype. For this purpose, we generated a null allele of *atg18* ($atg18^{\Delta}$). Removal of one copy of $atg18^{+}$ had no affect on NMJ growth in an otherwise wild-type background but significantly suppressed NMJ overgrowth caused by $atg1^{+}$ overexpression (Fig. 1, D and E). Removal of both copies of $atg18^{+}$ conferred almost complete suppression (Fig. 1, D and E). Therefore, NMJ overgrowth caused by $atg1^{+}$ overexpression is primarily caused by elevated levels of autophagy.

As a further test, we examined NMJ morphology after feeding larvae with rapamycin, which induces autophagy by inhibiting TOR (target of rapamycin), the key negative regulator of autophagy (Rubinsztein et al., 2007). Wild-type larvae fed rapamycin exhibited striking NMJ overgrowth similar to that caused by overexpressing $atg1^{+}$ (Fig. 1, D and F), which is consistent with the results of Knox et al. (2007). Rapamycin-induced NMJ overgrowth was completely suppressed by mutations in *atg18* (Fig. 1, D and F). Collectively, these results demonstrate that autophagy is a key positive regulator of NMJ growth.

Wairkar et al. (2009) observed NMJ undergrowth in *atg1* mutants but did not see overgrowth with $atg1^{+}$ overexpression. This discrepancy likely results from the use of different *UAS-atg1*$^{+}$ transgenes. For example, Wairkar et al. (2009) were only able to obtain partial (~50%) rescue of NMJ undergrowth in *atg1* mutants by overexpression of their *UAS-atg1*$^{rescue}$ construct, whereas we obtained complete rescue of this phenotype (Fig. S2).

### Atg1-mediated synaptic growth is independent of its nonautophagic functions

Atg1 has several functions unrelated to autophagy. We found that axonal transport is disrupted in *atg1*-null mutants (Fig. S1), which is a result also recently reported by Toda et al. (2008) and Wairkar et al. (2009). In addition, Atg1 suppresses translation by inhibiting the S6K kinase (Lee et al., 2007; Scott et al., 2007) and controls active zone density by inhibiting extracellular signal-regulated kinase (ERK) signaling (Wairkar et al., 2009). However, several lines of evidence indicate that these functions of Atg1 are not responsible for the NMJ phenotypes we observed when Atg1 activity was altered. First, *atg2* or *-18* mutants exhibited similar NMJ undergrowth but did not have defects in axonal transport (Fig. 1 A and Fig. S1). Thus, in agreement with Toda et al. (2008), we conclude that Atg1's role in axonal transport is distinct from its function in autophagy and NMJ growth. Second, blocking or activating translation by overexpressing a dominant-negative S6K transgene or constitutively activated S6K transgenes by *elav-Gal4* driver had little affect on NMJ growth (Fig. 2). Moreover, coexpression of any of the three constitutively activated S6K transgenes failed to suppress NMJ overgrowth caused by $atg1^{+}$ overexpression (Fig. 2). Thus, the role of Atg1 in S6K-dependent translation does not contribute to the NMJ phenotypes associated with manipulations of Atg1. Third, an ERK mutation does not affect NMJ growth. Although this ERK mutation suppresses the deficit in active zone density in *atg1* mutants, it does not suppress *atg1*'s NMJ undergrowth phenotype (Wairkar et al., 2009), indicating that it is not mediated by the ERK pathway. Collectively, these results demonstrate that altered levels of autophagy are primarily responsible for the effects of Atg1 on NMJ development.

### *wnd* and $bsk^{DN}$ suppress autophagy-dependent synaptic overgrowth

NMJ overgrowth induced by autophagy is distinctive and offers potential clues about pathways that may be involved. Formation of multiple long synaptic branches containing many small diameter boutons without any hyperbudding or satellite boutons most closely resembles the *hiw* phenotype (Wan et al., 2000), suggesting that autophagy and Hiw may function through the same pathway. Recent evidence indicates that Hiw inhibits NMJ growth by down-regulating Wnd, which in turn activates a Jun kinase encoded by *bsk* (*basket*). NMJ overgrowth in *hiw* is suppressed by mutations of *wnd* and by a dominant-negative mutation of *bsk* ($bsk^{DN}$; Collins et al., 2006). If the phenotypic similarity between *hiw* and increased autophagy reflects convergence on a common pathway, autophagy-induced NMJ overgrowth should also be suppressed by *wnd* and $bsk^{DN}$. Indeed, this is what we observed (Fig. 3). These results strongly support the idea that autophagy and Hiw converge on a Wnd-dependent MAPK signaling pathway to regulate NMJ development.

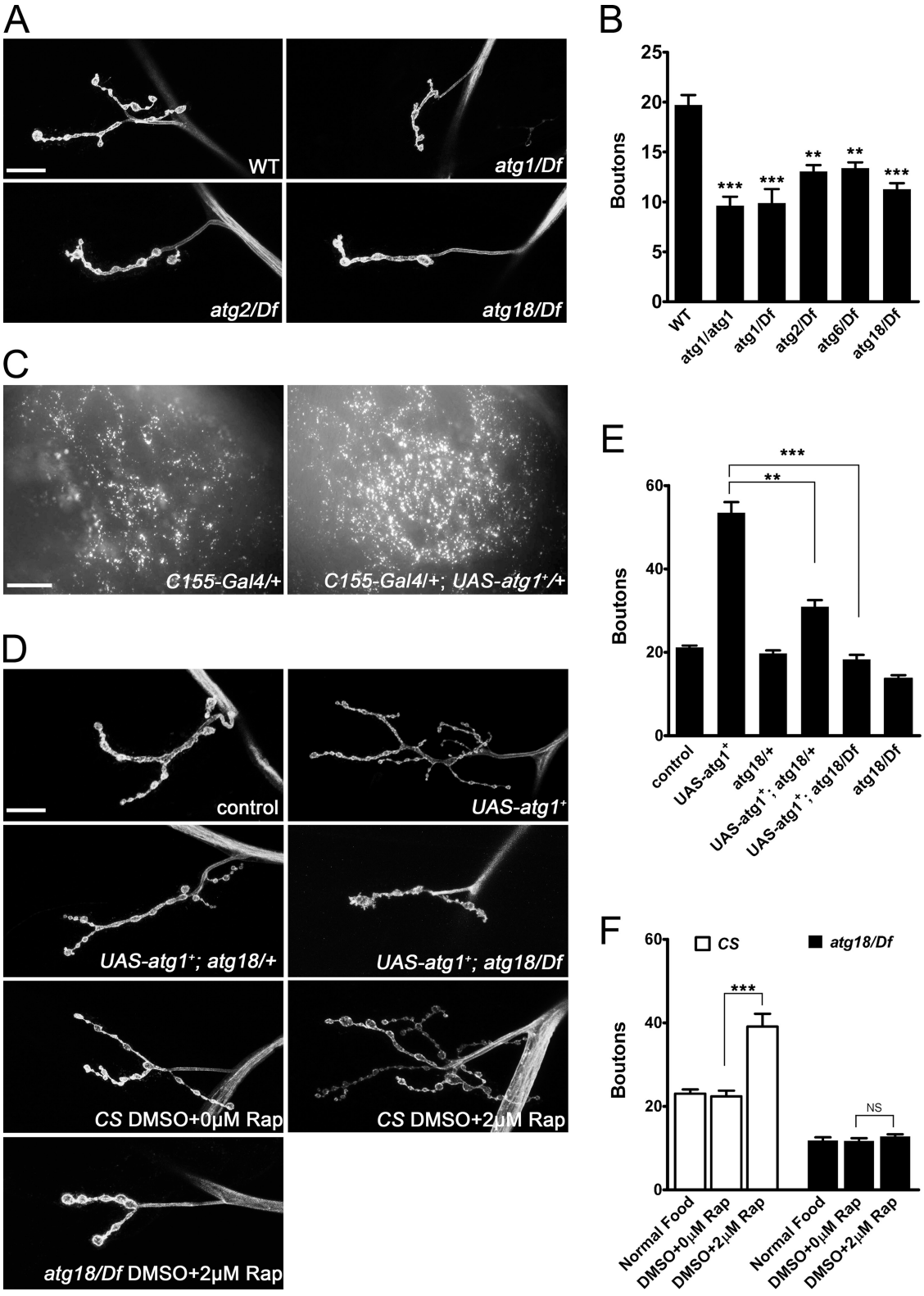


Figure 1. **Autophagy promotes NMJ growth in *Drosophila*.** (A) Confocal images of NMJ 4 labeled with FITC-HRP. Compared with control ($w^{1118}$), *atg1/Df*, *atg2/Df*, and *atg18/Df* mutants exhibit smaller NMJs. (B) Quantification of bouton numbers at NMJ 4 in larvae of the genotypes shown. (C) Fluorescent images of larval brain hemisphere of control (*C155-Gal4/+*) and *atg1*$^{+}$-overexpressing larvae (*C155-Gal4/UAS-atg1*$^{+}$) stained with LysoTracker. Substantially increased staining is observed in the latter, indicating elevated levels of autophagy. (D) Confocal images of NMJ 4 labeled with FITC-HRP. Compared with control (*elav-Gal4/+*), neuronal overexpression of *atg1*$^{+}$ (*UAS-atg1*$^{+}$) results in strong NMJ overgrowth. Overgrowth is reduced by loss of one copy of *atg18*$^{+}$ (*UAS-atg1*$^{+}$; *atg18/+*) and almost completely suppressed by removing both copies of *atg18*$^{+}$ (*UAS-atg1*$^{+}$; *atg18/Df*). Larvae fed on 2 μM rapamycin (Rap) to induce autophagy exhibit NMJ overgrowth, which is completely suppressed in an *atg18/Df* background. (E and F) Quantification of bouton numbers at NMJ 4 in the indicated larvae. (B, E, and F) Error bars denote SEM. **, $P < 0.01$; ***, $P < 0.001$. CS, Canton-S; WT, wild type. Bars: (A and D) 15 μm; (C) 50 μm.

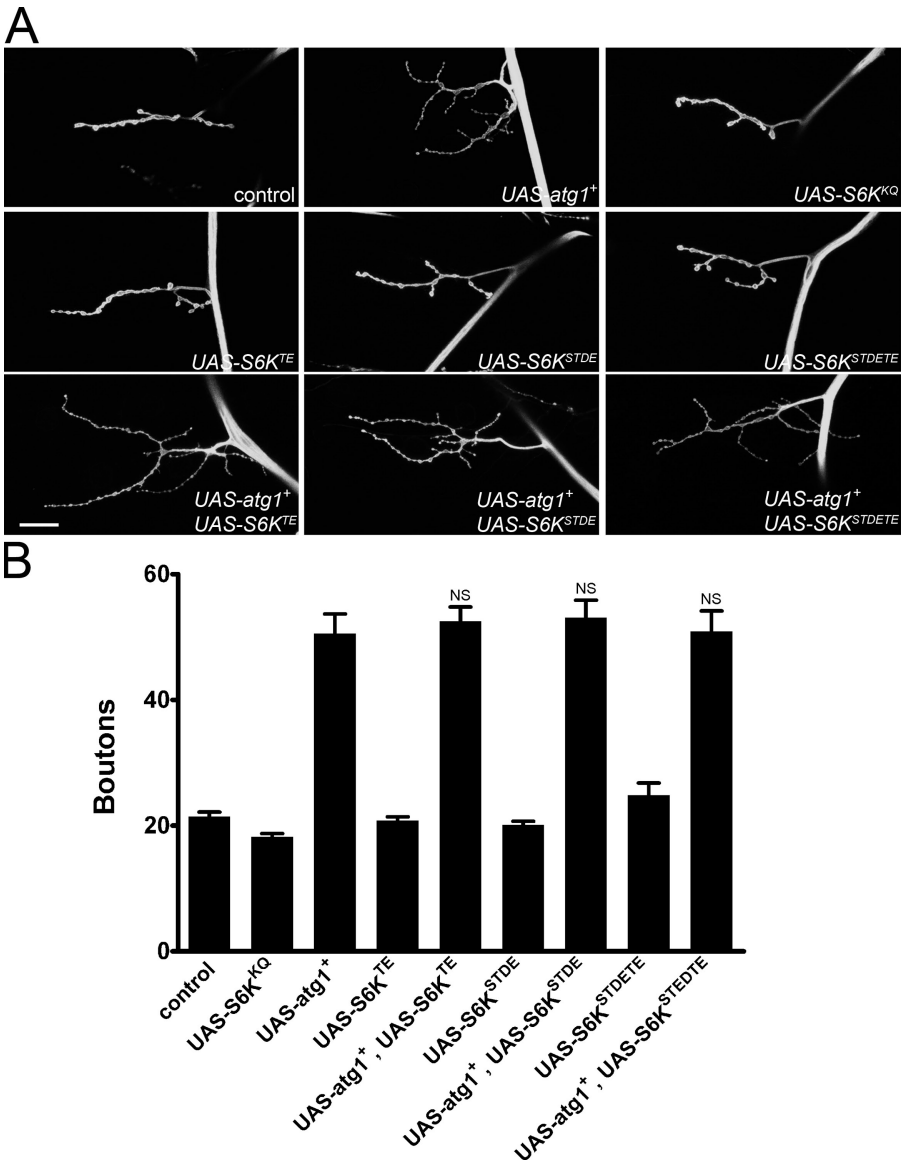


Figure 2. **Atg1-dependent changes in NMJ growth are independent of effects on translation.** (A) Confocal images of NMJ 4 labeled with FITC-HRP. Blocking or activating translation by overexpressing a dominant-negative S6K (*UAS-S6K*$^{KQ}$) or a constitutively activated S6K transgene (*UAS-S6K*$^{TE}$, *UAS-S6K*$^{STDE}$, or *UAS-S6K*$^{STDETE}$) has little affect on NMJ growth. None of three constitutively activated S6K transgenes suppresses NMJ overgrowth when coexpressed with *atg1*$^{+}$. (B) Quantification of bouton numbers at NMJ 4 in larvae of genotypes shown. Comparisons are made with *elav-Gal4/UAS-atg1*$^{+}$. Error bars denote SEM. Bar, 15 µm.

### Autophagy down-regulates Hiw

If autophagy and Hiw act via a common pathway, where do they converge? As a positive regulator of NMJ growth, autophagy could promote degradation of a negative regulator. An intriguing possibility is that Hiw is the negative regulator affected by autophagy. If a decrease in Hiw levels is responsible for NMJ overgrowth when autophagy is elevated, restoration of Hiw should suppress overgrowth. We tested this possibility by coexpressing wild-type Hiw with Atg1 and found that Atg1-mediated NMJ overgrowth was significantly suppressed (Fig. 4, A–D). This suppression is not simply an indirect consequence of the dilution of GAL4 caused by addition of a second UAS element because coexpression of *UAS-nwk*$^{+}$ did not suppress such NMJ overgrowth (Fig. 4 G). This result also shows that Nwk (Nervous wreck), another negative regulator of NMJ growth (Coyle et al. 2004), is not an apparent target of autophagy, as predicted by differences in phenotypes. Thus, autophagy appears to regulate NMJ growth through its effects on particular presynaptic proteins, and Hiw represents a key downstream effector.

To further test whether autophagy promotes NMJ growth by limiting Hiw, we eliminated one copy of *hiw*$^{+}$ to determine whether this further decrease in Hiw levels enhanced the effects of *atg1*$^{+}$ overexpression. In an otherwise wild-type background, loss of one copy of *hiw*$^{+}$ had no affect, but it significantly enhanced *atg1*$^{+}$-induced NMJ overgrowth (Fig. 4 G). The phenotype of *hiw* homozygotes overexpressing *atg1*$^{+}$ was no more extreme than *hiw* homozygote alone (Fig. 4, E–G). The absence of any additive or synergistic effects further supports the hypothesis that autophagy promotes NMJ development by down-regulating Hiw.

Because Hiw antibodies do not work for immunohistochemistry, we visualized Hiw using a fully functional GFP-tagged construct to test directly whether abundance of Hiw is affected by autophagy (Wu et al., 2005). In an otherwise wild-type background, Hiw-GFP was strongly expressed in neurons throughout the ventral ganglion and brain lobes driven by *C155-Gal4*, as detected by anti-GFP staining (Fig. 4, H1–H3). However, in larvae co-overexpressing *atg1*$^{+}$, the GFP signal

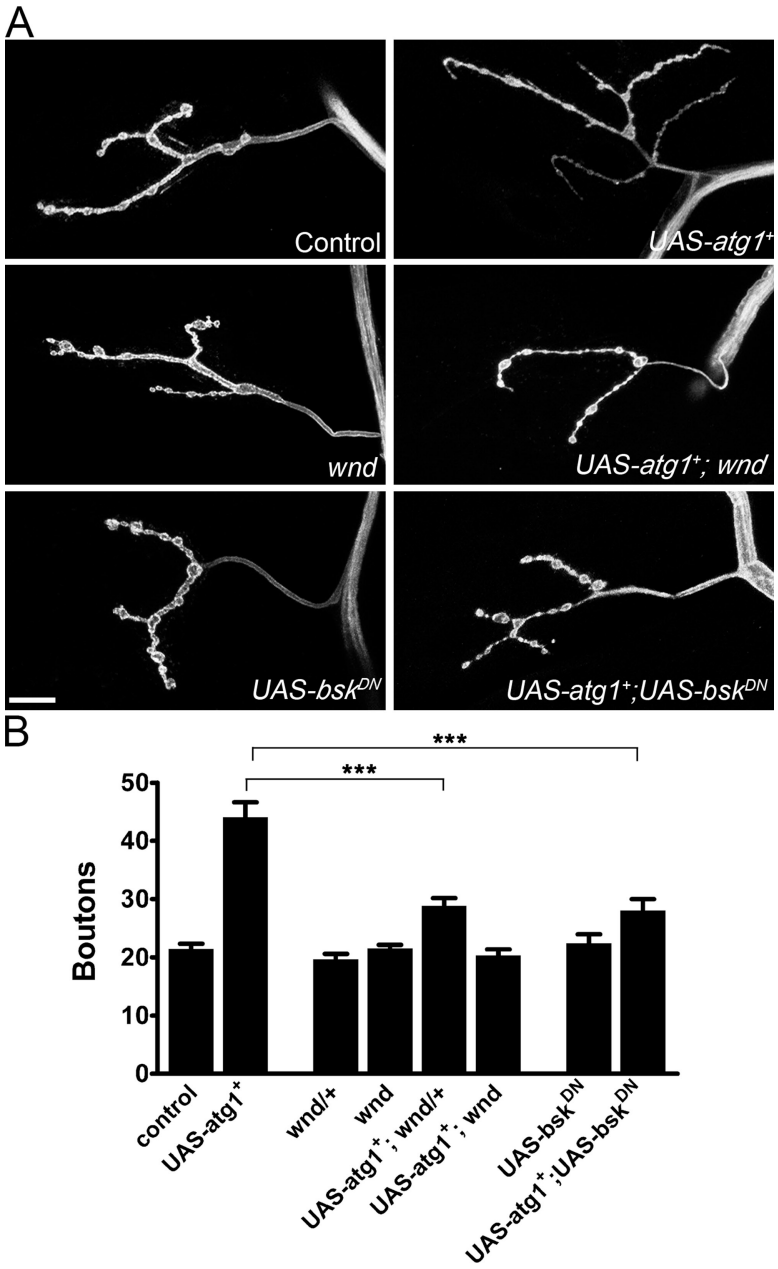


Figure 3. **Autophagy-dependent NMJ overgrowth is suppressed by *wnd* and *bsk*$^{DN}$.** (A) Confocal images of NMJ 4 labeled with FITC-HRP. Compared with control (*C155-Gal4/+*), neuronal overexpression of *atg1*$^{+}$ (*C155-Gal4/UAS-atg1*$^{+}$) results in NMJ overgrowth. Both *wnd* and *bsk*$^{DN}$ suppress NMJ overgrowth caused by *atg1*$^{+}$ overexpression. (B) Quantification of bouton numbers at NMJ 4 for larvae of genotypes shown. Error bars denote SEM. ***, P < 0.001. Bar, 15 µm.

was reduced by ~60% relative to anti-HRP staining (Fig. 4, I1–I3 and J). We confirmed this result by Western blot analysis (Fig. 4 K). Reduction of Hiw-GFP is not caused by the dilution of GAL4 by the presence of a second UAS element because coexpression of *UAS-myr-RFP* did not affect abundance of Hiw-GFP (Fig. 4 K). These results further indicate that autophagy promotes NMJ growth by down-regulating Hiw.

### Hiw-dependent synaptic undergrowth in *atg* mutants

Our results indicate that NMJ overgrowth caused by elevated autophagy is primarily caused by reduction in Hiw. Is the converse also true? Is NMJ undergrowth in *atg* mutants caused by elevated levels of Hiw? To address these questions, we expressed Hiw-GFP in neurons using *C155-Gal4* in various backgrounds. Hiw-GFP levels were significantly elevated in *atg1* and *-6* mutants compared with the controls, which is consistent with the idea that Hiw is down-regulated by autophagy (Fig. 5 A). If this increase in Hiw is a primary cause of NMJ undergrowth in *atg* loss-of-function mutants, eliminating Hiw should prevent this undergrowth; i.e., mutations in *hiw* should be epistatic to *atg* mutations. Thus, we examined NMJ morphology in *hiw*; *atg2* and *hiw*; *atg18* double mutants and found that *hiw* was completely epistatic (Fig. 5, B and C), demonstrating the role of elevated levels of Hiw in NMJ undergrowth of *atg* mutants.

A more direct test is to determine whether overexpression of Hiw can reduce NMJ size. However, this experiment is complicated because overexpression of Hiw by a relatively weak neuronal driver (*elav-Gal4*) does not affect NMJ size (Fig. 4), whereas overexpression of Hiw by a strong neuronal driver (*Elav-GeneSwitch*) has a modest dominant-negative effect (Wu et al., 2005). To determine whether increased levels of Hiw can

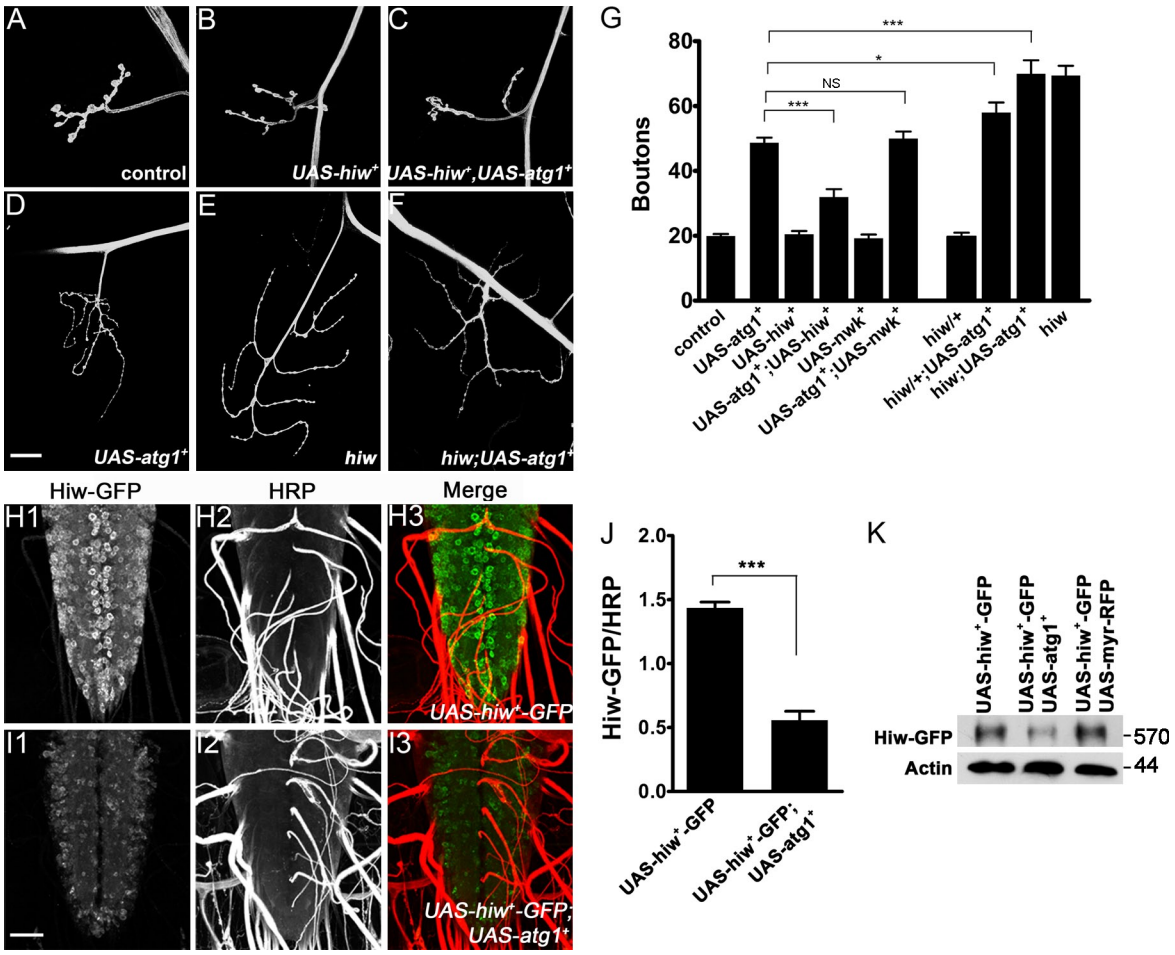


Figure 4. **Autophagy promotes synaptic growth via down-regulation of Hiw.** (A–F) Confocal images of NMJ 4 labeled with FITC-HRP. (A) *elav-Gal4/+*. (B–D) Neuronal overexpression of *hiw*$^+$ alone (B) via *elav-Gal4* driver has no affect on NMJ growth but is sufficient to suppress NMJ overgrowth caused by overexpression of *atg1*$^+$ (C and D). (E and F) Neuronal overexpression of *atg1*$^+$ in a *hiw* mutant background (F) does not further enhance NMJ growth compared with *hiw* mutants alone (E). (G) Quantification of bouton numbers at NMJ 4 in larvae of the genotypes shown. Comparisons are made with *elav-Gal4/UAS-atg1*$^+$. (H and I) Confocal images of larval ventral ganglia expressing a Hiw-GFP fusion protein labeled with anti-GFP (H1 and I1) and anti-HRP (H2 and I2). Hiw-GFP fusion protein is present at high levels in *C155-Gal4/UAS-hiw*$^+$*-GFP* larvae (H1–H3). However, Hiw levels are reduced by coexpression of *atg1*$^+$ in *C155-Gal4/UAS-hiw*$^+$*-GFP*; *UAS-atg1*$^+$ larvae (I1–I3), whereas HRP levels remain unchanged. (J) Quantification of Hiw-GFP and HRP fluorescence intensities in *C155-Gal4/UAS-hiw*$^+$*-GFP* larvae (1.44 ± 0.05; *n* = 4) and in *C155-Gal4/UAS-hiw*$^+$*-GFP*; *UAS-atg1*$^+$ larvae (0.55 ± 0.07; *n* = 5). (K) Western blots of extracts from larval brains probed for Hiw-GFP and actin confirm the reduction of Hiw-GFP levels caused by overexpression of *atg1*$^+$. Molecular mass is indicated in kilodaltons. (G and J) Error bars denote SEM. *, P < 0.05; ***, P < 0.001. Bars: (A–F) 25 µm; (H and I) 50 µm.

limit NMJ growth, it appears necessary to overexpress Hiw at an intermediate level. Therefore, we examined NMJs in larvae overexpressing *UAS-hiw*$^+$ via *C155-Gal4*. *C155-Gal4/+*; *UAS-hiw*$^+$*/+* female larvae exhibited very mild NMJ undergrowth (Fig. 5, D and E). Stronger undergrowth was observed in *C155-Gal4/Y*; *UAS-hiw*$^+$*/+* male larvae (Fig. 5, D and E). This difference is consistent with higher levels of *C155-Gal4* expression in males than in females, owing to dosage compensation (Warrick et al., 1999; Long and Griffith, 2000). We did not observe differences in NMJ growth between *C155-Gal4/+* female and *C155-Gal4/Y* male larvae, indicating that the undergrowth phenotypes are dependent on the levels of Hiw overexpression and not on differences in gender or expression of GAL4 alone (Fig. 5 D). Thus, moderate increases in Hiw levels result in NMJ undergrowth. Furthermore, the modest NMJ undergrowth in *C155-Gal4/+*; *UAS-hiw*$^+$*/+* larvae was enhanced when one copy of *atg1*$^+$, *-2*$^+$, or *-6*$^+$ was removed (Fig. 5, D and E). Together, these results indicate that elevated levels of Hiw account for most of the NMJ undergrowth in *atg* mutants. However, excess Hiw cannot fully explain NMJ undergrowth in *atg* mutants because NMJ undergrowth caused by Hiw overexpression is less severe than that of *atg1* and *-18* mutants. Thus, when autophagy is impaired, additional negative regulators may accumulate to depress NMJ growth. It is also likely that elevated levels of Hiw target proteins other than Wnd to limit synaptic growth because loss-of-function mutations of *wnd* do not affect NMJ development (Collins et al., 2006).

Because autophagy is generally thought of as a nonselective bulk degradation process, the idea that autophagy regulates NMJ growth primarily through its effects on Hiw levels seems difficult to understand at first. However, recent studies demonstrate that autophagy can also operate in a substrate-selective mode in regulating specific developmental events (Rowland et al., 2006; Zhang et al., 2009). For example, in *Caenorhabditis*

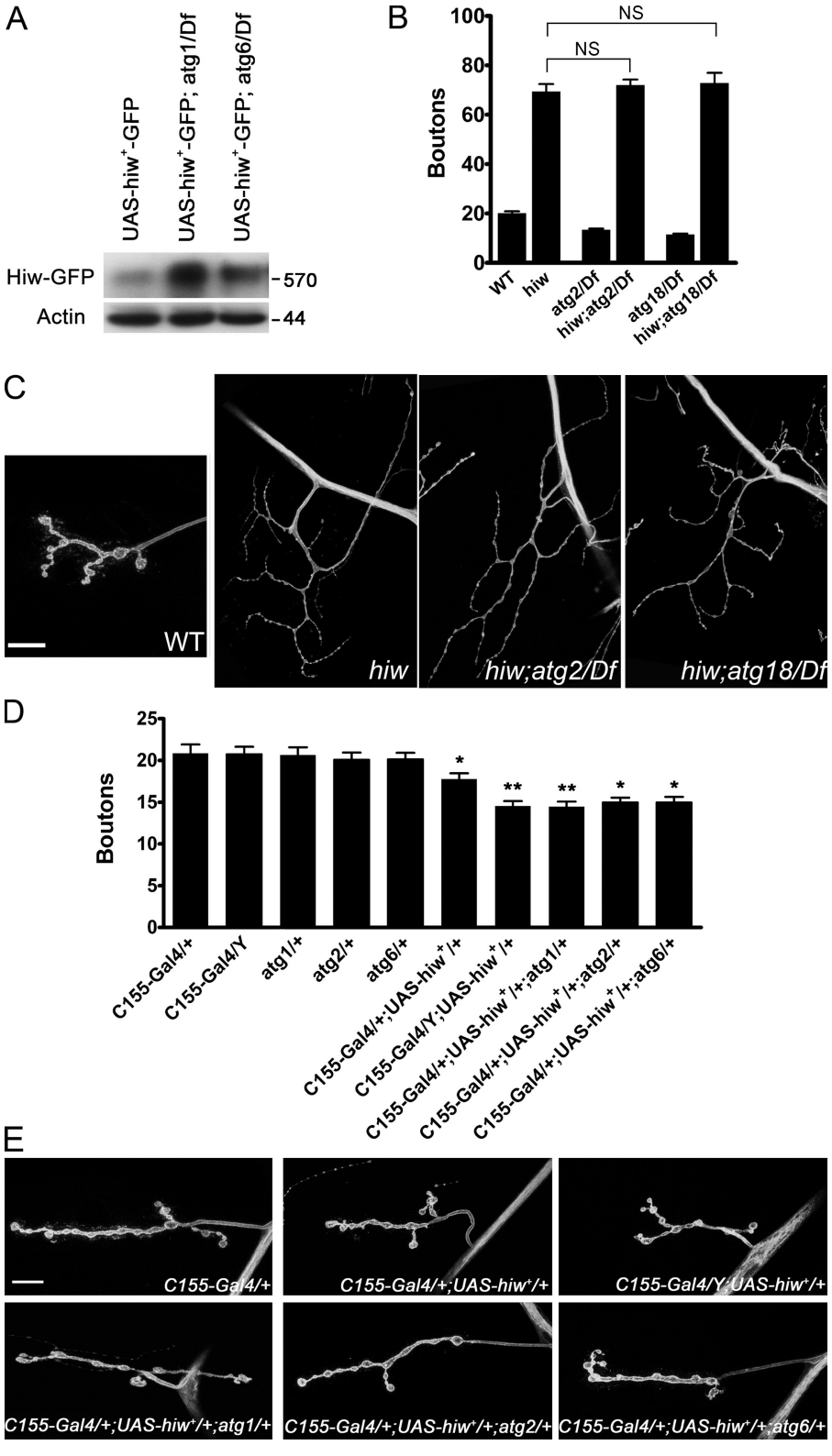


Figure 5. **Accumulation of Hiw contributes to NMJ undergrowth when autophagy is impaired.** (A) Western blots of larval brain extracts from the indicated genotypes probed for Hiw-GFP and actin show significant increases of Hiw-GFP levels in *atg1/Df* and *atg6/Df* mutants. Molecular mass is indicated in kilodaltons. (B) Quantification of bouton numbers at NMJ 4 in larvae of the genotypes shown. (C) Confocal images of NMJ 4 labeled with FITC-HRP. *hiw; atg2/Df* and *hiw; atg18/Df* NMJ overgrowth in double mutants is the same as *hiw* alone, which is consistent with the idea that Hiw is down-regulated by autophagy. (D) Quantification of bouton numbers at NMJ 4 in larvae of the genotypes shown. (E) Confocal images of NMJ 4 labeled with FITC-HRP. Moderate overexpression of Hiw in *C155-Gal4/+* females results in mild NMJ undergrowth. Stronger overexpression of Hiw in *C155-Gal4/Y* males leads to more marked NMJ undergrowth. When Hiw is overexpressed, loss of one copy of *atg1*$^{+}$, *-2*$^{+}$, or *-6*$^{+}$ further exacerbates NMJ undergrowth. (B and D) Error bars denote SEM. *, $P < 0.05$; **, $P < 0.01$. Bars: (C) 25 µm; (E) 15 µm.

*elegans*, when postsynaptic cells fail to receive presynaptic contact, $GABA_A$ receptors selectively traffic to autophagosomes (Rowland et al., 2006). However, the detailed mechanism of such selectivity is unknown. Zhang et al. (2009) identified SEPA-1 as a bridge that mediates the specific recognition and degradation of P granules by autophagy in *C. elegans* (Zhang et al., 2009). Thus, one possibility is that Hiw is specifically targeted to autophagosomes via a mechanism that remains to be elucidated. It is also possible that many presynaptic proteins besides Hiw are degraded by autophagy, but it is the reduction in Hiw that primarily affects NMJ size. Moreover, although we favor the idea that autophagy regulates Hiw directly, we cannot

rule out the possibility that autophagy promotes degradation of Hiw through an indirect mechanism involving the proteasome or other pathway.

In principle, autophagy could be acting on either side of the NMJ to regulate its development. Because *atg1*$^{+}$ overexpression in muscle results in lethality at the first larval instar, we are unable to assess whether this affects NMJ growth. Although we cannot rule out a postsynaptic role of autophagy in NMJ development, several results suggest that the effects of autophagy are primarily presynaptic: neuronal expression of *UAS-atg1*$^{+}$ is sufficient to completely rescue the NMJ undergrowth in *atg1* mutants (Fig. S2), the Hiw–Wnd pathway functions presynaptically (Wu et al., 2005; Collins et al., 2006), and *hiw* is completely epistatic to autophagy for NMJ growth.

Autophagy is of particular interest as a regulator of synaptic growth because it is triggered in response to many environmental cues. Our results demonstrate that decreasing or increasing autophagy from basal levels results in corresponding effects on synaptic size. Thus, autophagy is perfectly positioned to link environmental conditions with synaptic growth and plasticity. As such, it is intriguing to speculate on a role for autophagy in learning and memory.

## Materials and methods

### Fly stocks

Canton-S was used as a wild-type control. $w^{1118}$ was used as a control for genetic background. $atg1^{\Delta 3D}$, $UAS\text{-}atg1^{6A}$, and $UAS\text{-}atg1^{6B}$ (Scott et al., 2007) were provided by T. Neufeld (University of Minnesota, Minneapolis, MN). $hiw^{EMS}$, $UAS\text{-}hiw^{+}$, $UAS\text{-}hiw^{+}\text{-}GFP$, $wnd^{1}$, $wnd^{2}$ (Wan et al., 2000; Wu et al., 2005; Collins et al., 2006), and *elav-Gal4* were provided by A. DiAntonio (Washington University, St. Louis, MO). The following fly lines were obtained from the Bloomington Stock Center: $atg2^{EP3697}$, $atg18^{KG03090}$, $atg6^{l(3)00096}$, $UAS\text{-}bsk^{DN}$, $UAS\text{-}S6K^{STDE}$, $UAS\text{-}S6K^{STDETE}$, $UAS\text{-}S6K^{TE}$, $UAS\text{-}S6K^{KQ}$ (Spradling et al., 1999; Weber et al., 2000; Barcelo and Stewart, 2002; Scott et al., 2004; Berry and Baehrecke, 2007), *Df(3L)Exel6112*, *Df(3L)Exel6091*, *Df(3R)Exel6197*, and *Df(3L)BSC10*.

### Generation of $atg18^{\Delta}$ mutant in *Drosophila*

*P* element KG03090 was inserted within the first exon of the *atg18* gene, 127 bp upstream of the ATG start codon. $atg18^{\Delta}$ was generated by imprecise excision, which deletes 585 bp downstream of the KG03090 insertion site, removing the second exon, including the start codon, and part of the third exon. The $atg18^{\Delta}/Df$ mutant exhibited an NMJ undergrowth phenotype identical to $atg18^{KG03090}/Df$.

### Immunohistochemistry

Wandering third instar larvae were dissected in $Ca^{2+}$-free saline and fixed in 4% paraformaldehyde for 20 min. Larvae were incubated in primary antibodies overnight at 4°C or for 2 h at room temperature and in secondary antibodies for 1–2 h at room temperature and then mounted in Vectashield (Vector Laboratories) for microscopic analysis. For bouton quantification, we used rabbit anti-Nwk at 1:1,000 (Coyle et al., 2004) or rabbit anti–synaptotagmin I at 1:1,000 (H. Bellen, Baylor College of Medicine, Houston, TX). To detect Hiw-GFP fusion protein, mouse anti-GFP was used at 1:200 (Invitrogen). Specific secondary antibodies conjugated to Alexa Fluor 488, 568, and 647 (Invitrogen) were used at 1:200. Fluorescence-conjugated anti-HRP (Jackson ImmunoResearch Laboratories, Inc.) antibodies were used at 1:100.

### LysoTracker staining

Brains from *C155-Gal4/+* or *C155-Gal4/UAS-atg1*$^{+}$ third instar larvae were dissected in HL3 saline, incubated for 5 min in 0.1 µM LysoTracker red DND-99 (Invitrogen) in HL3 saline, rinsed twice in PBS and transferred to glass slides, and imaged immediately with a camera (Retiga 2000F; QImaging) mounted on a microscope (Optiphot-2; Nikon) using QCapture Pro 6.0 software (QImaging). All samples were processed and imaged under identical conditions.

### Imaging and quantification

We focused on NMJ 4 because of its relative simplicity; however, comparable results were also observed at NMJ 6/7 as well as at other NMJs we examined in mutant larvae. Quantification of bouton number was performed at NMJ 4 in segments A2–A4 as described previously (Coyle et al., 2004). Bouton numbers for each genotype are summarized in Table S1. The muscle size of all larvae analyzed was similar. Samples for each experiment were processed simultaneously with corresponding controls and imaged using the same confocal gain settings. Confocal images were obtained on a microscope (LSM 510; Carl Zeiss, Inc.) with Plan-Apochromat 20× NA 10.8, EC Plan-Neofluar 40× NA 1.3 oil differential interference contrast, or Plan-Apochromat 63× NA 1.4 oil differential interference contrast objectives and the accompanying software. Images were processed in LSM image browser (Carl Zeiss, Inc.) or ImageJ (National Institutes of Health). All images were captured at room temperature. For quantification of levels of Hiw-GFP, the total fluorescence of GFP immunoreactivity in the ventral ganglion was measured by ImageJ and standardized by total florescence of HRP in the same area. Statistical analyses were performed via analysis of variance and Tukey's or Dunnett's tests for multiple comparisons. Significance levels of $<0.05$, $<0.01$, or $<0.001$ are indicated by single, double, and triple asterisks, respectively, in the figures. Error bars denote SEM.

### Western blotting

Approximately 20 larval brains of each genotype were collected and homogenized on ice with 20 µl of homogenization buffer (67 mM Tris-HCl, pH 8.0, 67 mM NaCl, 2 M urea, 1.3% SDS, 2 mM DTT, and 1 mM EDTA; Wu et al., 2005). After adding SDS loading buffer, the homogenate was boiled for 10 min. The volume of six brains was loaded for each sample onto a two-layer SDS-PAGE gel with 5% upper layer and 12% lower layer. Western blots were probed with rabbit anti-GFP at 1:500 (Invitrogen) or goat antiactin at 1:1,000 (Santa Cruz Biotechnology, Inc.).

### Rapamycin treatment

30 female and 30 male flies were allowed to mate on standard laboratory fly food for 2–3 d and then transferred onto grape juice plates to lay eggs for 2–3 h. 40 embryos were collected and placed on standard laboratory food supplemented with DMSO alone or 2 µM rapamycin (LC Laboratories) dissolved in DMSO. Third instar larvae of each treatment were dissected and stained with anti–synaptotagmin I and FITC-HRP for bouton quantification.

### Online supplemental material

Fig. S1 shows that *atg1* mutants have axonal transport defects not seen in other autophagy mutants. Fig. S2 shows that NMJ undergrowth in *atg1* mutants is rescued by presynaptic expression of an *atg1*$^{+}$ transgene. Table S1 presents quantification of bouton numbers for each genotype. Online supplemental material is available at http://www.jcb.org/cgi/content/full/jcb.200907109/DC1.

We are particularly grateful to Thomas Neufeld for providing many of the fly strains used in these experiments along with much valuable information. We also thank Aaron DiAntonio, Hugo Bellen, and the Bloomington Stock Center for providing antibodies and fly lines. We are grateful to all members of the Ganetzky laboratory for helpful discussion and critical comments on the manuscript.

This research was supported by a predoctoral fellowship (0910048G) from the American Heart Association to W. Shen and a National Institutes of Health grant (NS15390) to B. Ganetzky.

Submitted: 17 July 2009
Accepted: 27 August 2009

## References

Aberle, H., A.P. Haghighi, R.D. Fetter, B.D. McCabe, T.R. Magalhães, and C.S. Goodman. 2002. wishful thinking encodes a BMP type II receptor that regulates synaptic growth in *Drosophila*. *Neuron*. 33:545–558. doi:10.1016/S0896-6273(02)00589-5

Barcelo, H., and M.J. Stewart. 2002. Altering *Drosophila* S6 kinase activity is consistent with a role for S6 kinase in growth. *Genesis*. 34:83–85. doi:10.1002/gene.10132

Berry, D.L., and E.H. Baehrecke. 2007. Growth arrest and autophagy are required for salivary gland cell degradation in *Drosophila*. *Cell*. 131:1137–1148. doi:10.1016/j.cell.2007.10.048

Collins, C.A., and A. DiAntonio. 2007. Synaptic development: insights from *Drosophila*. *Curr. Opin. Neurobiol.* 17:35–42. doi:10.1016/j.conb.2007.01.001

Collins, C.A., Y.P. Wairkar, S.L. Johnson, and A. DiAntonio. 2006. Highwire restrains synaptic growth by attenuating a MAP kinase signal. *Neuron*. 51:57–69. doi:10.1016/j.neuron.2006.05.026

Coyle, I.P., Y.H. Koh, W.C. Lee, J. Slind, T. Fergestad, J.T. Littleton, and B. Ganetzky. 2004. Nervous wreck, an SH3 adaptor protein that interacts with Wsp, regulates synaptic growth in *Drosophila*. *Neuron*. 41:521–534. doi:10.1016/S0896-6273(04)00016-9

Dickman, D.K., Z. Lu, I.A. Meinertzhagen, and T.L. Schwarz. 2006. Altered synaptic development and active zone spacing in endocytosis mutants. *Curr. Biol.* 16:591–598. doi:10.1016/j.cub.2006.02.058

Hara, T., K. Nakamura, M. Matsui, A. Yamamoto, Y. Nakahara, R. Suzuki-Migishima, M. Yokoyama, K. Mishima, I. Saito, H. Okano, and N. Mizushima. 2006. Suppression of basal autophagy in neural cells causes neurodegenerative disease in mice. *Nature*. 441:885–889. doi:10.1038/nature04724

Knox, S., H. Ge, B.D. Dimitroff, Y. Ren, K.A. Howe, A.M. Arsham, M.C. Easterday, T.P. Neufeld, M.B. O'Connor, and S.B. Selleck. 2007. Mechanisms of TSC-mediated control of synapse assembly and axon guidance. *PLoS One*. 2:e375. doi:10.1371/journal.pone.0000375

Koh, T.W., P. Verstreken, and H.J. Bellen. 2004. Dap160/intersectin acts as a stabilizing scaffold required for synaptic development and vesicle endocytosis. *Neuron*. 43:193–205. doi:10.1016/j.neuron.2004.06.029

Lee, S.B., S. Kim, J. Lee, J. Park, G. Lee, Y. Kim, J.M. Kim, and J. Chung. 2007. ATG1, an autophagy regulator, inhibits cell growth by negatively regulating S6 kinase. *EMBO Rep.* 8:360–365. doi:10.1038/sj.embor.7400917

Levine, B., and D.J. Klionsky. 2004. Development by self-digestion: molecular mechanisms and biological functions of autophagy. *Dev. Cell*. 6:463–477. doi:10.1016/S1534-5807(04)00099-1

Levine, B., and G. Kroemer. 2008. Autophagy in the pathogenesis of disease. *Cell*. 132:27–42. doi:10.1016/j.cell.2007.12.018

Liebl, F.L., Y. Wu, D.E. Featherstone, J.N. Noordermeer, L. Fradkin, and H. Hing. 2008. Derailed regulates development of the *Drosophila* neuromuscular junction. *Dev. Neurobiol.* 68:152–165. doi:10.1002/dneu.20562

Long, X., and L.C. Griffith. 2000. Identification and characterization of a SUMO-1 conjugation system that modifies neuronal calcium/calmodulin-dependent protein kinase II in *Drosophila melanogaster*. *J. Biol. Chem.* 275:40765–40776. doi:10.1074/jbc.M003949200

Marie, B., S.T. Sweeney, K.E. Poskanzer, J. Roos, R.B. Kelly, and G.W. Davis. 2004. Dap160/intersectin scaffolds the periactive zone to achieve high-fidelity endocytosis and normal synaptic growth. *Neuron*. 43:207–219. doi:10.1016/j.neuron.2004.07.001

Nakai, A., O. Yamaguchi, T. Takeda, Y. Higuchi, S. Hikoso, M. Taniike, S. Omiya, I. Mizote, Y. Matsumura, M. Asahi, et al. 2007. The role of autophagy in cardiomyocytes in the basal state and in response to hemodynamic stress. *Nat. Med.* 13:619–624. doi:10.1038/nm1574

O'Connor-Giles, K.M., L.L. Ho, and B. Ganetzky. 2008. Nervous wreck interacts with thickveins and the endocytic machinery to attenuate retrograde BMP signaling during synaptic growth. *Neuron*. 58:507–518. doi:10.1016/j.neuron.2008.03.007

Pack-Chung, E., P.T. Kurshan, D.K. Dickman, and T.L. Schwarz. 2007. A *Drosophila* kinesin required for synaptic bouton formation and synaptic vesicle transport. *Nat. Neurosci.* 10:980–989. doi:10.1038/nn1936

Packard, M., E.S. Koo, M. Gorczyca, J. Sharpe, S. Cumberledge, and V. Budnik. 2002. The *Drosophila* Wnt, wingless, provides an essential signal for pre- and postsynaptic differentiation. *Cell*. 111:319–330. doi:10.1016/S0092-8674(02)01047-4

Rodal, A.A., R.N. Motola-Barnes, and J.T. Littleton. 2008. Nervous wreck and Cdc42 cooperate to regulate endocytic actin assembly during synaptic growth. *J. Neurosci.* 28:8316–8325. doi:10.1523/JNEUROSCI.2304-08.2008

Rowland, A.M., J.E. Richmond, J.G. Olsen, D.H. Hall, and B.A. Bamber. 2006. Presynaptic terminals independently regulate synaptic clustering and autophagy of GABAA receptors in *Caenorhabditis elegans*. *J. Neurosci.* 26:1711–1720. doi:10.1523/JNEUROSCI.2279-05.2006

Rubinsztein, D.C., J.E. Gestwicki, L.O. Murphy, and D.J. Klionsky. 2007. Potential therapeutic applications of autophagy. *Nat. Rev. Drug Discov.* 6:304–312. doi:10.1038/nrd2272

Schuster, C.M., G.W. Davis, R.D. Fetter, and C.S. Goodman. 1996. Genetic dissection of structural and functional components of synaptic plasticity. I. Fasciclin II controls synaptic stabilization and growth. *Neuron*. 17:641–654. doi:10.1016/S0896-6273(00)80197-X

Scott, R.C., O. Schuldiner, and T.P. Neufeld. 2004. Role and regulation of starvation-induced autophagy in the *Drosophila* fat body. *Dev. Cell*. 7:167–178. doi:10.1016/j.devcel.2004.07.009

Scott, R.C., G. Juhász, and T.P. Neufeld. 2007. Direct induction of autophagy by Atg1 inhibits cell growth and induces apoptotic cell death. *Curr. Biol.* 17:1–11. doi:10.1016/j.cub.2006.10.053

Spradling, A.C., D. Stern, A. Beaton, E.J. Rhem, T. Laverty, N. Mozden, S. Misra, and G.M. Rubin. 1999. The Berkeley Drosophila Genome Project gene disruption project: Single P-element insertions mutating 25% of vital *Drosophila* genes. *Genetics*. 153:135–177.

Toda, H., H. Mochizuki, R. Flores III, R. Josowitz, T.B. Krasieva, V.J. Lamorte, E. Suzuki, J.G. Gindhart, K. Furukubo-Tokunaga, and T. Tomoda. 2008. UNC-51/ATG1 kinase regulates axonal transport by mediating motor-cargo assembly. *Genes Dev.* 22:3292–3307. doi:10.1101/gad.1734608

Wairkar, Y.P., H. Toda, H. Mochizuki, K. Furukubo-Tokunaga, T. Tomoda, and A. Diantonio. 2009. Unc-51 controls active zone density and protein composition by downregulating ERK signaling. *J. Neurosci.* 29:517–528. doi:10.1523/JNEUROSCI.3848-08.2009

Wan, H.I., A. DiAntonio, R.D. Fetter, K. Bergstrom, R. Strauss, and C.S. Goodman. 2000. Highwire regulates synaptic growth in *Drosophila*. *Neuron*. 26:313–329. doi:10.1016/S0896-6273(00)81166-6

Warrick, J.M., H.Y. Chan, G.L. Gray-Board, Y. Chai, H.L. Paulson, and N.M. Bonini. 1999. Suppression of polyglutamine-mediated neurodegeneration in *Drosophila* by the molecular chaperone HSP70. *Nat. Genet.* 23:425–428. doi:10.1038/70532

Weber, U., N. Paricio, and M. Mlodzik. 2000. Jun mediates Frizzled-induced R3/R4 cell fate distinction and planar polarity determination in the *Drosophila* eye. *Development*. 127:3619–3629.

Wu, C., Y.P. Wairkar, C.A. Collins, and A. DiAntonio. 2005. Highwire function at the *Drosophila* neuromuscular junction: spatial, structural, and temporal requirements. *J. Neurosci.* 25:9557–9566. doi:10.1523/JNEUROSCI.2532-05.2005

Zhang, Y., L. Yan, Z. Zhou, P. Yang, E. Tian, K. Zhang, Y. Zhao, Z. Li, B. Song, J. Han, et al. 2009. SEPA-1 mediates the specific recognition and degradation of P granule components by autophagy in *C. elegans*. *Cell*. 136:308–321. doi:10.1016/j.cell.2008.12.022